High-Fidelity Indirect Readout of Trapped-Ion Hyperfine Qubits

Stephen D. Erickson,[1,2,*] Jenny J. Wu,[1,2] Pan-Yu Hou,[1,2] Daniel C. Cole,[1] Shawn Geller,[1,2] Alex Kwiatkowski,[1,2] Scott Glancy,[1] Emanuel Knill,[1,3] Daniel H. Slichter,[1] Andrew C. Wilson,[1] and Dietrich Leibfried[1,†]

[1]*National Institute of Standards and Technology, 325 Broadway, Boulder, Colorado 80305, USA*
[2]*Department of Physics, University of Colorado, Boulder, Colorado 80309, USA*
[3]*Center for Theory of Quantum Matter, University of Colorado, Boulder, Colorado 80309, USA*

(Received 12 December 2021; accepted 17 March 2022; published 21 April 2022)

We propose and demonstrate a protocol for high-fidelity indirect readout of trapped ion hyperfine qubits, where the state of a $^{9}Be^{+}$ qubit ion is mapped to a $^{25}Mg^{+}$ readout ion using laser-driven Raman transitions. By partitioning the $^{9}Be^{+}$ ground-state hyperfine manifold into two subspaces representing the two qubit states and choosing appropriate laser parameters, the protocol can be made robust to spontaneous photon scattering errors on the Raman transitions, enabling repetition for increased readout fidelity. We demonstrate combined readout and back-action errors for the two subspaces of $1.2^{+1.1}_{-0.6} \times 10^{-4}$ and $0^{+1.9}_{-0} \times 10^{-5}$ with 68% confidence while avoiding decoherence of spectator qubits due to stray resonant light that is inherent to direct fluorescence detection.

DOI: 10.1103/PhysRevLett.128.160503

Trapped ions are a leading platform for quantum information processing (QIP), exhibiting high fidelities in state preparation and measurement [1–7], single-qubit rotations [3,8], and two-qubit entangling gates [9–12], as well as promising pathways to scalability [13–15]. High fidelity demonstrations have involved one or a few qubits at a time. As QIP systems grow beyond tens of qubits [16–19], undesirable crosstalk on neighboring "spectator" qubits can be harmful, particularly for fault-tolerant quantum error correction protocols [20–22].

In trapped ion QIP, absorption of resonant photons by spectator ions can cause crosstalk; a single such photon absorbed by a spectator ion will destroy any quantum information encoded in its internal state [23,24]. This has measurable impact on circuits that incorporate mid-circuit measurement [25–27], though significantly lower crosstalk has been demonstrated in specific systems [28]. Reduced resonant light crosstalk will be an essential requirement for large-scale fault-tolerant QIP with atomic qubits. Techniques such as quantum logic spectroscopy (QLS) [29], where information about the state of a qubit is mapped via a shared motional mode to a different species of ion for fluorescence detection, achieve this by only using photons that are far off-resonant from qubit ions [30,31]. Thereby, QLS avoids resonant light crosstalk at the cost of mixed-species quantum logic. Ions of a second species are already used for sympathetic cooling in large quantum algorithms with trapped ions [32].

QLS-based readout has the potential to be quantum nondemolition (QND), where the state of the qubit is unchanged by the measurement process after initial projection and, thus, can be repeated to increase readout fidelity. In practice, measurements never fulfill this ideal, and the number of times they can be repeated while still improving the overall readout fidelity is limited. Reference [33] demonstrated 6×10^{-4} infidelity for reading out an $^{27}Al^{+}$ optical clock qubit through repetitive QLS, ultimately limited by the 21 s lifetime of the $^{3}P_0$ qubit state.

In this Letter, we extend repetitive indirect readout to hyperfine qubits in ions with nuclear spin $\geq 3/2$ in a way that is resilient to off-resonant photon scattering errors, demonstrate approximately an order of magnitude lower average indirect readout infidelity than in previous experiments with ions, and develop a rigorous statistical analysis for readout using repeated measurements. We contain spontaneous photon scattering from the qubit Raman lasers within orthogonal subspaces by tailoring the laser beam intensities and polarizations, thereby, ensuring that state-changing scattering events do not cause transitions between subspaces. Analogous subspace resilience to photon loss when reading out superconducting cavity qubits has been demonstrated [34]. We propose two variants for reading out a $^{9}Be^{+}$ qubit using a cotrapped $^{25}Mg^{+}$ readout ion [Fig. 1(a)] and demonstrate the one that is compatible with our apparatus.

The $^{2}S_{1/2}$ ground state of $^{9}Be^{+}$, with states labeled $|F, m_F\rangle$, is divided into two orthogonal subspaces defined as $S_{+} \equiv \{|F, m_F \geq 1\rangle\}$ and $S_{-} \equiv \{|F, m_F \leq 0\rangle\}$. The QLS scheme uses two-photon stimulated Raman transitions [13] that are designed to keep the qubit within a single subspace as shown in Fig. 1(b).

The $\Delta m_F = 0$ variant of the scheme, represented by dashed red lines in Fig. 1, uses two σ^{+}-polarized Raman

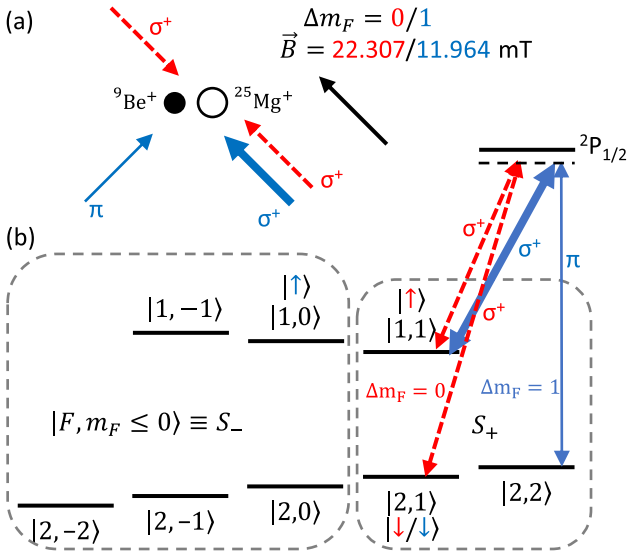

FIG. 1. (a) Raman beam polarizations and geometries using either of two proposed variants ($\Delta m_F = 0$ in dashed red, $\Delta m_F = 1$ in solid blue). Magnetic fields are chosen to provide a field-insensitive qubit transition that can be driven with the same set of Raman laser beams. (b) Subspaces within the $^9Be^{+2}S_{1/2}$ ground states and associated field-insensitive qubit states (color coded) for either configuration. Line thickness varies between Raman beams to indicate relative intensities.

beams, ideally with equal intensity, to drive the $|F = 2, m_F = 1\rangle \leftrightarrow |1, 1\rangle$ transition for QLS. A good qubit choice is the same $|2, 1\rangle \leftrightarrow |1, 1\rangle$ transition that is first-order insensitive to magnetic fields at an applied field of $|\vec{B}| \approx 22.307$ mT. Before readout, $|\uparrow\rangle \equiv |1, 1\rangle$ could be transferred to S_-, ideally to $|2, -2\rangle$. With the use of composite pulse sequences and multiple shelving states in S_-, high shelving fidelity should be readily achievable, though imperfections in this process will increase readout error. The choice of Raman beam polarizations closes S_+ under any off-resonant scattering, allowing for many QLS repetitions. Transitions from S_+ to S_- require a Raman beam polarization error, and transitions from S_- to S_+ require multiple off-resonant scattering events given a successful initial transfer to $|2, -2\rangle$.

An alternative variant, shown in solid blue in Fig. 1(b), drives $\Delta m_F = 1$ transitions with a strong σ^+ and a weak π-polarized Raman beam. This is compatible with QLS on $|2, 2\rangle \leftrightarrow |1, 1\rangle$ and computation on the $|2, 1\rangle \leftrightarrow |1, 0\rangle$ qubit transition, which is first-order field-insensitive for $|\vec{B}| \approx 11.964$ mT and couples to the same Raman beam polarizations. Consequently, prior to readout, one would transfer $|1, 0\rangle \rightarrow |2, -2\rangle$ and $|2, 1\rangle \rightarrow |2, 2\rangle$. The $\Delta m_F = 1$ variant retains most of the benefit of the $\Delta m_F = 0$ variant, except that the π-polarized Raman beam opens an additional pathway to transition from S_+ to S_-. Its intensity should be kept low to reduce this rate. We consider the $\Delta m_F = 0$ variant superior to the $\Delta m_F = 1$ variant due to the improved subspace preservation and more efficient use of Raman beam power of the former. However, due to limitations on the magnetic field strength and Raman beam geometry in our apparatus, we demonstrate the $\Delta m_F = 1$ variant.

Since subspace preservation in either variant depends on the Raman scattering rate of the qubit ion, it is desirable to choose ion coupling parameters that minimize that rate, possibly even at the expense of single-repetition QLS fidelity. This implies working with the highest feasible Raman beam detuning from excited states. The sideband coupling rate is proportional to the Lamb-Dicke (LD) parameter, so further benefit can be obtained by maximizing the $^9Be^+$ LD parameter through choice of confining well, motional mode, and Raman beam wave vector difference. To this end, we operate on the $^9Be^+ - {}^{25}Mg^+$ crystal axial out-of-phase mode at 2.91 MHz, with $^9Be^+$ and $^{25}Mg^+$ LD parameters of 0.37 and 0.097, respectively. Techniques based on the Mølmer-Sørensen interaction [35–39] could offer higher single-repetition QLS fidelity, but likely come with increased spontaneous Raman scattering, so we use temperature-sensitive sideband-based QLS [29].

During readout, information is transferred from the $^{25}Be^+$ qubit ion, through the motional mode, to the $^{25}Mg^+$ readout ion with a qubit ion blue sideband (BSB, $|2, 2\rangle \otimes |n\rangle \leftrightarrow |1, 1\rangle \otimes |n + 1\rangle$) or red sideband (RSB, $|2, 2\rangle \otimes |n\rangle \leftrightarrow |1, 1\rangle \otimes |n - 1\rangle$) π pulse followed by a readout ion RSB π pulse. After the transfer, the state of the readout ion is determined using standard state-dependent fluorescence detection [40]. The scheme is designed to pump any density matrix population in S_+ into the state $|2, 2\rangle$ and to leave any population in S_- undisturbed. The full protocol is shown in Fig. 2 and detailed below.

At the start of each trial, we optically pump to $|2, 2\rangle$, followed by microwave composite pulse transfer to $|2, -2\rangle$ if S_- is desired. Because of imperfections in this process, two sequences of the repetitive QLS protocol are performed back-to-back, the first of which heralds subspace preparation for the second.

At the start of each QLS repetition, we perform a crystallization check by detecting readout ion fluorescence to ensure that the ions are cooled to near the Doppler limit, indicated by the resulting photon count number being above a set threshold. If the photon counts are below the threshold, this check fails and additional cooling is applied to the readout ion to attempt recrystallization, followed by a second crystallization check. Then, we ground state cool the collective motion through the readout ion and reprepare the readout ion. Next, we apply a qubit ion BSB π pulse that creates a phonon in the motional mode if the qubit ion is in $|2, 2\rangle$ and transfers $|2, 2\rangle$ to $|1, 1\rangle$. If the qubit ion was not in $|2, 2\rangle$, this operation is ideally off resonant from any other allowable transition from the motional ground state, and no phonons are injected. A readout-ion RSB π pulse and fluorescence detection then probes whether a phonon was injected. Again, we ground state cool and reprepare the readout ion. Then, we apply an RSB π pulse to the qubit ion

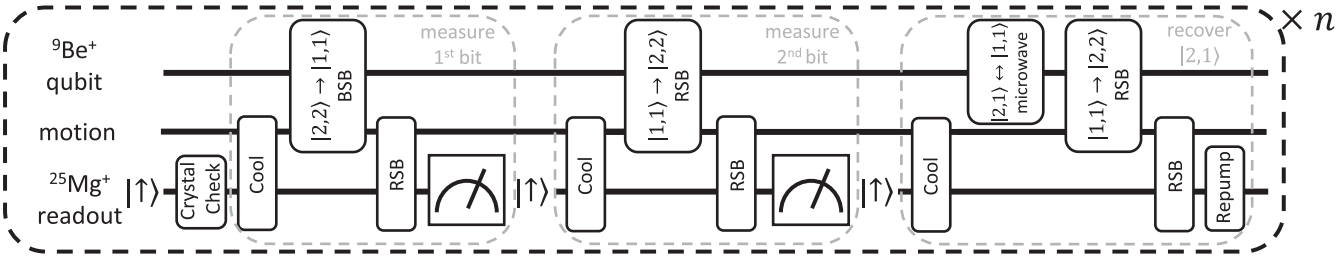

FIG. 2. Circuit for one repetition of the QLS protocol, which can be repeated n times for higher fidelity. Sidebands on the ^{9}Be$^+$ qubit inject phonons into the collective out-of-phase motional mode if in S_+. These phonons are detected by the ^{25}Mg$^+$ readout ion sidebands and subsequent fluorescence detections, yielding two bits of information per repetition. Leaked density matrix population from the ^{9}Be$^+$ $|2,1\rangle$ state is then recovered.

that creates a phonon if the qubit ion was in $|1,1\rangle$ and transfers $|1,1\rangle$ to $|2,2\rangle$. Again, the presence of a created phonon is detected using a readout ion RSB pulse and fluorescence detection. Then, we cool and reprepare the readout ion.

The binary outcomes of the two fluorescence detections depend on the initial state of the qubit ion, taking nominal values of (1,1) for initial state $|2,2\rangle$, (0,1) for initial state $|1,1\rangle$, and (0,0) for initial states in S_- or $|2,1\rangle$. Thus, population in $|2,1\rangle$ can cause readout errors.

To avoid remaining in $|2,1\rangle$, in the last stage of each repetition, we use a microwave π pulse to transfer any population in $|2,1\rangle$ to $|1,1\rangle$, and then to $|2,2\rangle$ with a RSB π pulse. Given that scattering to $|2,1\rangle$ is expected to be a rare occurrence, rather than detecting whether a phonon was injected (which would indicate that the qubit had likely been in $|2,1\rangle$), we simply cool it away. With this strategy, although population in $|2,1\rangle$ can cause an error during a single repetition, any population in $|2,1\rangle$ is unlikely to persist through multiple QLS repetitions. The $\Delta m_F = 0$ variant would be done similarly, except with the roles of $|2,2\rangle$ and $|2,1\rangle$ reversed.

This constitutes one full repetition of the QLS protocol, which can be repeated multiple times in a given trial to increase readout fidelity. The number of useful repetitions is limited by the increasing cumulative probability of $S_+ \leftrightarrow S_-$ transitions due to spontaneous Raman scattering from the qubit ion. Bayesian analysis is performed based on reference data to determine the posterior probability of being in a particular subspace given a sequence of QLS results, declaring the most probable result of the readout (see Supplemental Material [41], for details).

Since the readout infidelity is expected to be small compared to state preparation error during optical pumping, each trial consists of two sequences of repetitive QLS. The first sequence projectively prepares a subspace, which is heralded by the readout result of this sequence. The second sequence is applied without repreparing the qubit. If this second readout disagrees with the first, then, to lowest order either the second readout is in error or the first (heralding) readout correctly read out the initial qubit subspace, but changed it in the process (back-action error). We cannot distinguish these two effects, so readout infidelities we report are their sum (and, hence, an upper bound on each) to leading order. This leading order estimate is applied to the set of test data shown in Fig. 3. We compute bounds on higher order corrections to the leading order estimates, and use them for our main results presented in Table I [41]. The corrections are small compared to the statistical uncertainties on the leading order estimates.

To eliminate errors or bias due to brief failures of our apparatus, we discard any experimental trials where the apparatus failed a status check, such as due to an optical cavity losing lock, a failed interleaved crystallization check, or a failed fluorescence pre- or postcheck on either species [41]. This method of selecting valid trials in real time could be used in near-term devices to increase readout fidelity at the expense of lowering algorithm execution rates. Prior to each trial, we carry out a validation check by performing one repetition of QLS with the qubit prepared in each subspace in turn. Then, we track the fraction of the last 100 such validation checks that passed. If, at any point, either

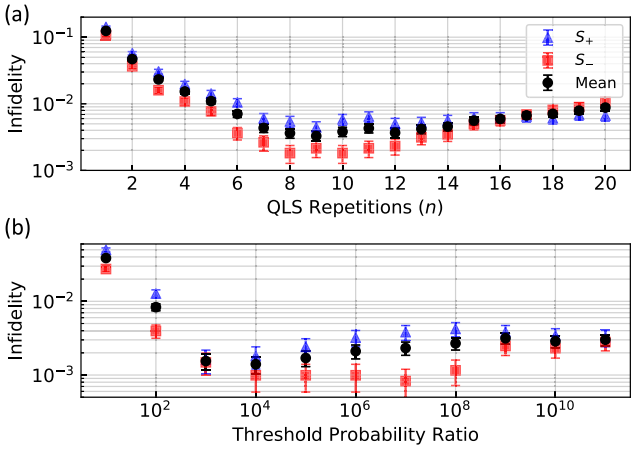

FIG. 3. Low-detuning (45 GHz) test data showing (a) infidelity of the readout protocol vs number of QLS repetitions per readout and (b) infidelity vs threshold probability ratio for adaptive readout that repeats QLS until a threshold is reached. Blue triangles are used for S_+ infidelity, red squares for S_-, and black circles for their mean. Error bars are 68% confidence intervals.

TABLE I. Infidelities (combined readout and back-action error) of the adaptive readout protocol at 68% confidence for different Raman beam detunings, Raman beam intensity ratios, threshold posterior probability ratio, and mean number of QLS repetitions needed to exceed that ratio.

Detuning (GHz)	Intensity ratio	Threshold ratio	Mean repetitions	S_+ infidelity	S_- infidelity
45	35:1	10^4	3.55	$2.7^{+0.6}_{-0.5} \times 10^{-3}$	$2^{+3}_{-2} \times 10^{-4}$
90	120:1	10^7	5.13	$8.1^{+4.2}_{-2.9} \times 10^{-4}$	$2.6^{+2.8}_{-1.8} \times 10^{-4}$
210	35:1	10^7	5.92	$2.5^{+1.3}_{-0.9} \times 10^{-4}$	$0^{+1.8}_{-0} \times 10^{-5}$
490	15:1	10^9	8.55	$1.2^{1.1}_{-0.6} \times 10^{-4}$	$0^{+1.9}_{-0} \times 10^{-5}$

fraction falls below a preset threshold, the entire 100-trial window is discarded. This guards against errors in the apparatus that are not caught by other validation checks, ensures that experiments where the apparatus fails are not erroneously counted as successfully reading out S_-, and protects against degradation of the QLS performance and, hence, the inferred fidelity of reading out S_+.

To demonstrate the basic features of the readout protocol, first, we collect a test dataset with Raman lasers 45 GHz red detuned from the $^2S_{1/2} \leftrightarrow {}^2P_{1/2}$ transition and a 35:1 intensity ratio between the two beams. For comparison, 900 GHz detuning was previously used for high-fidelity entangling gates with $^9Be^+$ [10]. The test data consist of 40 full repetitions of QLS per experiment. We analyzed different-sized subsets of this dataset in postprocessing, consisting of the first $2n$ repetitions for all values of n in the range $1 \leq n \leq 20$. In each subset, the first n repetitions are used to provide heralded state preparation, and the next n repetitions are used to determine readout fidelity. The resulting infidelities for reading out either subspace, and their mean, are shown in Fig. 3(a). The infidelity after one QLS repetition is relatively high, but decreases with additional repetitions, reaching a minimum mean infidelity of $3.3(6) \times 10^{-3}$ after nine repetitions. Then, it gradually rises due to the increasing cumulative probability of a subspace-changing spontaneous Raman scattering event.

We can substantially reduce the average number of repetitions by computing the posterior probability ratio of being in one subspace over the other, and stopping once the target ratio is reached, which may be different for each trial [41]. We refer to this as "adaptive readout" [1,28,33,43]. Figure 3(b) shows the infidelity achieved for a range of threshold probability ratios using the same 45 GHz test dataset, analyzed adaptively in postprocessing. An infidelity of $1.4(4) \times 10^{-3}$ is reached for a 10^4 probability ratio after an average of 3.47 repetitions, providing both an improvement in fidelity and a reduction in the average duration of the protocol compared to the optimal fixed number of repetitions.

We also perform an adaptive readout in real time on our experiment control field-programmable gate array for 45, 90, 210, and 490 GHz Raman detunings. The results are shown in Table I. To ensure that the infidelity only weakly depends on the threshold probability ratio, as observed in Fig. 3(b), and to guard against experimental drifts causing errors in the probability estimates, we set the threshold conservatively high. At each detuning, we made the Raman beam power imbalance as large as possible while keeping sideband π-pulse durations τ within the range $5\ \mu s \leq \tau \leq 40\ \mu s$. Shorter τ will drive carrier transitions off resonantly, while longer τ makes the π pulse fidelity more susceptible to drifts in the qubit or motional frequencies. We also require the π-polarized beam to be strong enough for feedback stabilization of pulse envelopes. The real time data at 45 GHz align with those of the post-processed test dataset, and infidelity decreases with detuning, ultimately reaching $1.2^{+1.1}_{-0.6} \times 10^{-4}$ and $0^{+1.9}_{-0} \times 10^{-5}$ infidelity at 68% confidence for S_+ and S_-, respectively, at 490 GHz detuning and a 15:1 intensity ratio ($1.2^{+2.39}_{-0.95} \times 10^{-4}$ and $0^{3.9}_{-0} \times 10^{-5}$ at 95% confidence). For comparison, at this detuning, the separately measured infidelity for reading out S_+ without the procedure for recovering population from $|2,1\rangle$ is $4(2) \times 10^{-4}$, and the average single-repetition Raman scattering probability within S_+ is $5(1) \times 10^{-4}$.

At detunings of 210 and 490 GHz, the infidelity in reading out S_- is small and difficult to quantify; since multiple spontaneous Raman scattering events are required for population beginning in $|2,-2\rangle$ within S_- to scatter into S_+, the probability of leaving S_- rapidly drops with the scattering rate. We observed no disagreements between the first and second readouts in roughly 100 000 experiments for reading out S_- in the 210 and 490 GHz datasets. On the other hand, the probability of changing from S_+ to S_- is given by a constant times the spontaneous Raman scattering rate. This proportionality constant is much less than 1, and depends on the strong σ^+-beam polarization error and Raman beam intensity ratio. Scattering out of S_+ could be reduced by using a qubit ion with larger nuclear spin where S_+ includes more states, and multiple scattering events would be required to exit the S_+ subspace. However, additional states must be incorporated into the protocol by adding appropriate repumping steps (analogous to the repumping of $|2,1\rangle$).

The duration of repeated QLS readouts, typically around 100 ms for the largest Raman detunings (14.7 ms per repetition, of which 7.1 ms was spent on optical pumping or Doppler cooling and 6.4 ms on sideband cooling), sets a

practical limit on the number of experimental trials and, thus, the statistical power for quantifying the S_- readout error. This duration is dominated by ground-state cooling, and could be substantially reduced using alternative sub-Doppler cooling techniques, for example, electromagnetically induced transparency cooling [44,45]. The next leading contributions are optical pumping and Doppler cooling durations, which could likely be shortened without major impact, and the fluorescence detection duration, which can be reduced by considering photon arrival times [1].

In conclusion, we demonstrate indirect qubit subspace readout of trapped ions with approximately an order of magnitude reduction in average infidelity relative to previous work [33]. The observed readout infidelities are competitive with the lowest readout infidelities (direct or indirect) of any qubit [1–7,34], and could be improved further with the $\Delta m_F = 0$ variant of the scheme. The protocol extends repetitive QND measurements to hyperfine qubits in a way that is resilient to spontaneous Raman scattering. Alternatively, such scattering could be avoided by using magnetic field gradients for spin-motion coupling, instead [13,46–48]. The scheme also effectively eliminates errors due to stray resonant laser light that can affect spectator qubits in large quantum processors. The technique can be used on any ion with nuclear spin $\geq 3/2$, with the possible addition of a tailored repumper to clear metastable D states, or any species with very long-lived excited states [5,6].

We thank Yu Liu and Matthew Bohman for helpful comments on the manuscript. S. D. E., J. J. W., P.-Y. H., S. G., and A. K. acknowledge support from the Professional Research Experience Program (PREP) operated jointly by NIST and the University of Colorado. S. D. E. acknowledges support from the a National Science Foundation Graduate Research Fellowship under Grant No. DGE 1650115. D. C. C. acknowledges support from a National Research Council Postdoctoral Fellowship. This work was supported by IARPA and the NIST Quantum Information Program.

*stephen.erickson@colorado.edu
†dietrich.leibfried@nist.gov

[1] A. H. Myerson, D. J. Szwer, S. C. Webster, D. T. C. Allcock, M. J. Curtis, G. Imreh, J. A. Sherman, D. N. Stacey, A. M. Steane, and D. M. Lucas, Phys. Rev. Lett. **100**, 200502 (2008).
[2] A. H. Burrell, D. J. Szwer, S. C. Webster, and D. M. Lucas, Phys. Rev. A **81**, 040302(R) (2010).
[3] T. P. Harty, D. T. C. Allcock, C. J. Ballance, L. Guidoni, H. A. Janacek, N. M. Linke, D. N. Stacey, and D. M. Lucas, Phys. Rev. Lett. **113**, 220501 (2014).
[4] J. E. Christensen, D. Hucul, W. C. Campbell, and E. R. Hudson, npj Quantum Inf. **6**, 35 (2020).
[5] C. L. Edmunds, T. R. Tan, A. R. Milne, A. Singh, M. J. Biercuk, and C. Hempel, Phys. Rev. A **104**, 012606 (2021).
[6] A. Ransford, C. Roman, T. Dellaert, P. McMillin, and W. C. Campbell, Phys. Rev. A **104**, L060402 (2021).
[7] L. A. Zhukas, P. Svihra, A. Nomerotski, and B. B. Blinov, Phys. Rev. A **103**, 062614 (2021).
[8] K. R. Brown, A. C. Wilson, Y. Colombe, C. Ospelkaus, A. M. Meier, E. Knill, D. Leibfried, and D. J. Wineland, Phys. Rev. A **84**, 030303(R) (2011).
[9] C. J. Ballance, T. P. Harty, N. M. Linke, M. A. Sepiol, and D. M. Lucas, Phys. Rev. Lett. **117**, 060504 (2016).
[10] J. P. Gaebler, T. R. Tan, Y. Lin, Y. Wan, R. Bowler, A. C. Keith, S. Glancy, K. Coakley, E. Knill, D. Leibfried, and D. J. Wineland, Phys. Rev. Lett. **117**, 060505 (2016).
[11] R. Srinivas, S. C. Burd, H. M. Knaack, R. T. Sutherland, A. Kwiatkowski, S. Glancy, E. Knill, D. J. Wineland, D. Leibfried, A. C. Wilson *et al.*, Nature (London) **597**, 209 (2021).
[12] C. R. Clark, H. N. Tinkey, B. C. Sawyer, A. M. Meier, K. A. Burkhardt, C. M. Seck, C. M. Shappert, N. D. Guise, C. E. Volin, S. D. Fallek, H. T. Hayden, W. G. Rellergert, and K. R. Brown, Phys. Rev. Lett. **127**, 130505 (2021).
[13] D. J. Wineland, C. Monroe, W. M. Itano, D. Leibfried, B. E. King, and D. M. Meekhof, J. Res. Natl. Inst. Stand. Technol. **103**, 259 (1998).
[14] D. Kielpinski, C. Monroe, and D. J. Wineland, Nature (London) **417**, 709 (2002).
[15] C. Monroe and J. Kim, Science **339**, 1164 (2013).
[16] N. Friis, O. Marty, C. Maier, C. Hempel, M. Holzäpfel, P. Jurcevic, M. B. Plenio, M. Huber, C. Roos, R. Blatt, and B. Lanyon, Phys. Rev. X **8**, 021012 (2018).
[17] K. Wright, K. M. Beck, S. Debnath, J. M. Amini, Y. Nam, N. Grzesiak, J.-S. Chen, N. C. Pisenti, M. Chmielewski, C. Collins *et al.*, Nat. Commun. **10**, 5464 (2019).
[18] F. Arute, K. Arya, R. Babbush, D. Bacon, J. C. Bardin, R. Barends, R. Biswas, S. Boixo, F. G. S. L. Brandao, D. A. Buell *et al.*, Nature (London) **574**, 505 (2019).
[19] C. E. Bradley, J. Randall, M. H. Abobeih, R. C. Berrevoets, M. J. Degen, M. A. Bakker, M. Markham, D. J. Twitchen, and T. H. Taminiau, Phys. Rev. X **9**, 031045 (2019).
[20] M. Sarovar, T. Proctor, K. Rudinger, K. Young, E. Nielsen, and R. Blume-Kohout, Quantum **4**, 321 (2020).
[21] P. Parrado-Rodríguez, C. Ryan-Anderson, A. Bermudez, and M. Müller, Quantum **5**, 487 (2021).
[22] P.-Y. Hou, L. He, F. Wang, X.-Z. Huang, W.-G. Zhang, X.-L. Ouyang, X. Wang, W.-Q. Lian, X.-Y. Chang, and L.-M. Duan, Chin. Phys. Lett. **36**, 100303 (2019).
[23] D. Leibfried, M. D. Barrett, A. B. Kish, J. Britton, J. Chiaverini, B. DeMarco, W. M. Itano, B. Jelenković, J. D. Jost, C. Langer *et al.*, in *Laser Spectroscopy* (World Scientific, Singapore, 2004), pp. 295–303.
[24] C. D. Bruzewicz, J. Chiaverini, R. McConnell, and J. M. Sage, Appl. Rev. Phys. **6**, 021314 (2019).
[25] Y. Wan, D. Kienzler, S. D. Erickson, K. H. Mayer, T. R. Tan, J. J. Wu, H. M. Vasconcelos, S. Glancy, E. Knill, D. J. Wineland *et al.*, Science **364**, 875 (2019).
[26] C. Ryan-Anderson, J. G. Bohnet, K. Lee, D. Gresh, A. Hankin, J. P. Gaebler, D. Francois, A. Chernoguzov, D. Lucchetti, N. C. Brown, T. M. Gatterman, S. K. Halit, K. Gilmore, J. A. Gerber, B. Neyenhuis, D. Hayes, and R. P. Stutz, Phys. Rev. X **11**, 041058 (2021).

[27] J. P. Gaebler, C. H. Baldwin, S. A. Moses, J. M. Dreiling, C. Figgatt, M. Foss-Feig, D. Hayes, and J. M. Pino, Phys. Rev. A **104**, 062440 (2021).
[28] S. Crain, C. Cahall, G. Vrijsen, E. E. Wollman, M. D. Shaw, V. B. Verma, S. W. Nam, and J. Kim, Commun. Phys. **2**, 97 (2019).
[29] P. O. Schmidt, T. Rosenband, C. Langer, W. M. Itano, J. C. Bergquist, and D. J. Wineland, Science **309**, 749 (2005).
[30] M. D. Barrett, B. DeMarco, T. Schaetz, V. Meyer, D. Leibfried, J. Britton, J. Chiaverini, W. M. Itano, B. Jelenković, J. D. Jost, C. Langer, T. Rosenband, and D. J. Wineland, Phys. Rev. A **68**, 042302 (2003).
[31] T. R. Tan, High-fidelity entangling gates with trapped-ions, Ph.D. thesis, University of Colorado at Boulder, 2016.
[32] J. M. Pino, J. M. Dreiling, C. Figgatt, J. P. Gaebler, S. A. Moses, M. S. Allman, C. H. Baldwin, M. Foss-Feig, D. Hayes, K. Mayer, C. Ryan-Anderson, and B. Neyenhuis, Nature (London) **592**, 209 (2021).
[33] D. B. Hume, T. Rosenband, and D. J. Wineland, Phys. Rev. Lett. **99**, 120502 (2007).
[34] S. S. Elder, C. S. Wang, P. Reinhold, C. T. Hann, K. S. Chou, B. J. Lester, S. Rosenblum, L. Frunzio, L. Jiang, and R. J. Schoelkopf, Phys. Rev. X **10**, 011001 (2020).
[35] A. Sørensen and K. Mølmer, Phys. Rev. Lett. **82**, 1971 (1999).
[36] T. R. Tan, J. P. Gaebler, Y. Lin, Y. Wan, R. Bowler, D. Leibfried, and D. J. Wineland, Nature (London) **528**, 380 (2015).
[37] C. D. Bruzewicz, R. McConnell, J. Stuart, J. M. Sage, and J. Chiaverini, npj Quantum Inf. **5**, 102 (2019).
[38] D. Kienzler, Y. Wan, S. D. Erickson, J. J. Wu, A. C. Wilson, D. J. Wineland, and D. Leibfried, Phys. Rev. X **10**, 021012 (2020).
[39] A. C. Hughes, V. M. Schäfer, K. Thirumalai, D. P. Nadlinger, S. R. Woodrow, D. M. Lucas, and C. J. Ballance, Phys. Rev. Lett. **125**, 080504 (2020).
[40] G. Janik, W. Nagourney, and H. Dehmelt, J. Opt. Soc. Am. B **2**, 1251 (1985).
[41] See Supplemental Material at http://link.aps.org/supplemental/10.1103/PhysRevLett.128.160503 for details on data analysis, which includes Ref. [42].
[42] C. J. Clopper and E. S. Pearson, Biometrika **26**, 404 (1934).
[43] S. L. Todaro, V. B. Verma, K. C. McCormick, D. T. C. Allcock, R. P. Mirin, D. J. Wineland, S. W. Nam, A. C. Wilson, D. Leibfried, and D. H. Slichter, Phys. Rev. Lett. **126**, 010501 (2021).
[44] C. F. Roos, D. Leibfried, A. Mundt, F. Schmidt-Kaler, J. Eschner, and R. Blatt, Phys. Rev. Lett. **85**, 5547 (2000).
[45] Y. Lin, J. P. Gaebler, T. R. Tan, R. Bowler, J. D. Jost, D. Leibfried, and D. J. Wineland, Phys. Rev. Lett. **110**, 153002 (2013).
[46] F. Mintert and C. Wunderlich, Phys. Rev. Lett. **87**, 257904 (2001).
[47] C. Ospelkaus, U. Warring, Y. Colombe, K. R. Brown, J. M. Amini, D. Leibfried, and D. J. Wineland, Nature (London) **476**, 181 (2011).
[48] R. Srinivas, S. C. Burd, R. T. Sutherland, A. C. Wilson, D. J. Wineland, D. Leibfried, D. T. C. Allcock, and D. H. Slichter, Phys. Rev. Lett. **122**, 163201 (2019).